Available online at www.sciencedirect.com

ScienceDirect

Materials Today: Proceedings 4 (2017) 5006–5012

www.materialstoday.com/proceedings

The Living Light Conference 2016

Vapor sensing using a bio-inspired porous silicon photonic crystal☆

Jonathan Rasson[a]*, Olivier Poncelet[a], Sébastien R. Mouchet[b,c], Olivier Deparis[b], Laurent A. Francis[a]**

[a]*Institute of Information and Communication Technologies, Electronics and Applied Mathematics, Université catholique de Louvain, Place du Levant 3, 1348 Louvain-la-Neuve, Belgium*

[b]*Department of Physics, Physics of Matter and Radiation (PMR), University of Namur, rue de Bruxelles 61, 5000 Namur, Belgium*

[c]*College of Engineering, Mathematics and Physical Sciences, University of Exeter, Stocker Road, Exeter EX4 4QL, United Kingdom*

Abstract

Naturally occurring photonic crystals present on the wing scales of *Papilio* butterflies are known to exhibit vivid iridescent coloration as well as various optical properties, including vapor sensing properties. This work reports the fabrication of a periodic array of concave multilayers in porous silicon mimicking the *Papilio blumei* nanostructure and its application as an optical vapor sensor. We compared the variations in the reflectance spectrum due to ethanol vapor adsorption and condensation inside the bio-inspired concave porous silicon multilayer structure to the variations of a standard flat porous silicon Bragg mirror. This results in an enhanced response time in the case of the bio-inspired concave structure.

Selection and Peer-review under responsibility of The Living Light Conference (May 4 – 6) 2016, San Diego (USA).

Keywords: porous silicon; Papilio butterfly, photonic crystal; vapor sensor; optical detection; biomimetism; ethanol vapor

1. Introduction

When looking for nanostructures exhibiting specific properties having potential real world applications, it is often useful to study what Nature has to offer. For instance, the scales of butterfly wings possessing iridescent structural colors are based on photonic nanostructures that exhibit numerous interesting properties. Among those

* Main corresponding author. Tel.: +3210472174.

E-mail address: jonathan.rasson@uclouvain.be

** Corresponding author. Tel.: +3210473533; fax: +3210472598.

E-mail address: laurent.francis@uclouvain.be

Selection and Peer-review under responsibility of The Living Light Conference (May 4 – 6) 2016, San Diego (USA).

properties, the response to change of the refractive index of the ambient environment is very valuable as it leads to the possibility to use these structures as a vapor sensing platform. Based on this observation, butterflies from the *Morpho* family have been extensively studied for their sensitivity to various vapors [1-5]. Multiple researches have hence been conducted to develop techniques to reproduce the scales nanostructure, known as a Christmas tree-like architecture, based either on bio-templating [6-14] or bottom-up approaches using micro-fabrication techniques [15-25].

Even though the majority of vapor sensing studies, based on naturally occurring butterfly nanostructures, have been conducted on *Morpho*, Wang *et al.* recently demonstrated that the concave multilayer structure of the *Papilio blumei* (Fig. 1) shows an increased response to change of refractive index due to contact with liquids compared to *Morpho* [26]. The concave multilayer structure of the butterflies from the *Papilio* family has been widely studied for its optical properties [27-30]. This led to studies aiming at reproducing this structure on a larger scale. The methods used for the bio-templating approach are the atomic layer deposition (ALD) of oxides [31] and the sol-gel templating [32-34]. Another approach used is the bottom-up approach where the *Papilio*-like structure has been replicated either using colloids [35-37] or a combination of standard micro-fabrication techniques and ALD oxides [38]. Nevertheless, this structure has never been reproduced up to now for vapor sensing applications.

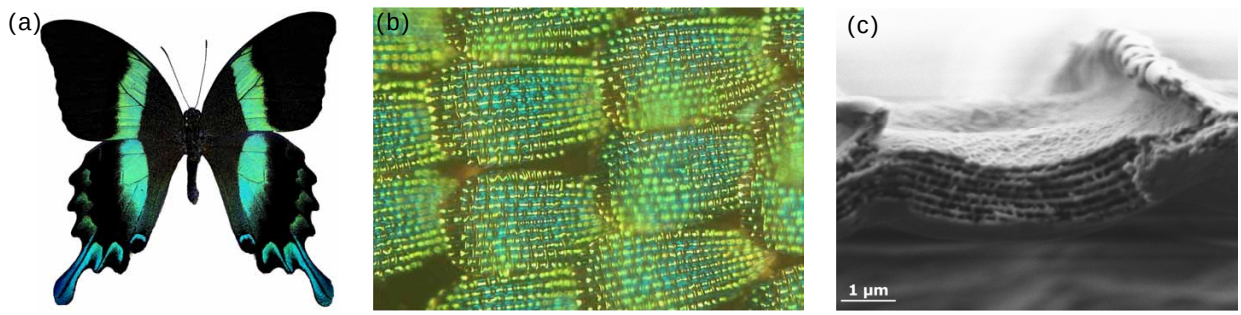

Fig. 1. (a) Picture of a *Papilio blumei* butterfly. (b) Optical microscope picture of the scales of a *Papilio blumei*. (c) Scanning Electron Microscope (SEM) picture of the cross section of a *Papilio blumei*'s scale.

In this work we suggest the use of porous silicon to reproduce the concave multilayer structure of *P. blumei*. Indeed, porous silicon is an interesting material due to its versatility as well as its porosity leading to a high surface/volume ratio (up to 500 m^2/cm^3) and therefore to an increased sensitivity to chemical volatile species. Based on these properties, the use of porous silicon substrates has been largely reported for the detection of various kinds of chemical species [39-44]. Among those, most optical detection schemes are based on the use of multilayered porous silicon Bragg mirrors for the detection of volatile organic compounds [45-47].

We fabricated a flat porous silicon Bragg mirror, acting as the standard for vapor sensing using porous silicon in order to compare its optical response to changes in the surrounding environment, due to the exposure to ethanol vapors to the one of the bio-inspired structure.

2. Materials and Methods

2.1 Processes

Both the bio-inspired concave porous silicon multilayer structure and flat Bragg mirror were produced using p-type boron-doped (100) silicon wafers with a resistivity of 0.8-1.2 mΩ.cm (Sil'Tronix Silicon Technologies, France). For the fabrication of the concave porous silicon multilayer, a 400 nm silicon oxide layer was deposited on the wafers by wet oxidation. Photolithography was then performed to pattern networks with slits of 1 µm and steps of 20 µm in photoresist (AZ 6612, Chem-Lab, Belgium). The oxide mask was then opened using buffered HF (7:1 NH_4F:HF) to expose the silicon and the photoresist was stripped by oxygen plasma. The cavities were afterwards etched in the silicon by wet etching using an HNA solution, a chemical solution composed of fluorhydric acid (HF 49%, Chem-Lab), nitric acid (HNO_3 70%, Chem-Lab), and glacial acetic acid (CH_3COOH 99-100%, Chem-Lab) with a ratio of 3:94:3 v/v [38]. Finally the oxide mask was removed in BHF 7:1. Structured wafers and non-

processed wafers were then electrochemically etched to produce the concave multilayer and the flat Bragg mirror, respectively. The electrochemical etching was performed using a potentiostat/galvanostat (PGSTAT302N from Metrohm Belgium nv, Belgium) as the current source and a custom-made single-bath Teflon cell. The silicon was porosified in an HF:ethanol electrolyte (3:1 v/v, HF 49% from Chem-Lab and ethanol absolute from VWR Chemicals, Belgium). Two current densities were applied to obtain different porosities, the porosity increasing with the current density, which led to two optical indices. Each electrochemical etching cycle was composed of two current density steps of 12.5 and 80 mA/cm^2 applied for 9.3 and 2.5 seconds respectively. The cycle was repeated 10 times to obtain a 20 layers multilayer.

2.2 Optical measurements under vapor flow

Both the flat Bragg mirror and the bio-inspired concave multilayer were optically characterized in a sealed stainless steel chamber in the presence of ethanol vapor (Fig. 2). The pressure inside the chamber was maintained at 1.030 bar by a pressure controller in order to prevent any leaks. The samples were introduced inside the chamber and their reflectance was recorded by a spectrophotometer (AvaSpec-ULS2048-2-USB2, Avantes, Netherlands) with optical fibers held in place using an optical fiber holder (AFH-15, Avantes). For each measurement, the specular reflectance was thus measured at a 15° angle with respect to the normal to the sample surface using a xenon lamp (AvaLight-Xe, Avantes) as the light source. The measurements were normalized by a reference measurement recorded on a spectralon (RS-2, Avantes).

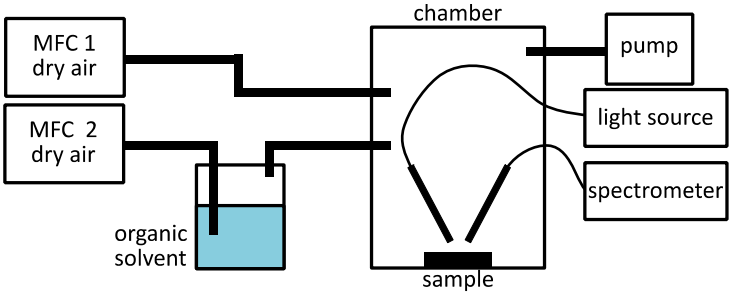

Fig. 2. Experimental set-up used for the optical detection of ethanol vapor.

The injected vapor flow, coming from a bubbler, was controlled using a mass flow controller (MFC, Bronkhorst High-Tech EL-FLOW select) and diluted with dry air (Air Liquide Alphagaz, $N_2 + O_2 \geq 99.999\%$). The total flow of vapor and dry air was set to 200 sccm, the dilutions used in the vapor sensing experiments are presented in Table 1, with 0% corresponding to pure dry air and 100% to saturated vapor. It is to be noted that the ethanol concentration or relative pressure cannot be estimated because the relative pressure of the ethanol vapor in the flow coming from the bubbler cannot be assumed to be 100% since the liquid vaporization does not occur at equilibrium. The chamber was vacuum-purged before each measurement in order to evacuate vapors from the experimental set-up and the sample. After each increase in vapor concentration, a 5-minute delay was established before recording the optical spectrum of the sample. Further details about the optical characterization set-up are available in [15,48].

Table 1.Vapor dilutions used during the measurements.

Vapor [sccm]	Dry air [sccm]	100*Vap./tot.flow [%]
0	200	0
50	150	25
100	100	50
150	50	75
200	0	100

3. Results and discussion

3.1 Concave porous silicon multilayer structure

From previous results of silicon etching using HNA, hemispherical cavities are expected due to the isotropic etching properties of the HNA etchant [38]. However, we observe an anisotropic feature in the cavities of the bio-inspired porous silicon structure (Fig. 3): a profile separated in two different regimes. On one hand, the top of the cavities is curved, which would be expected for an entirely isotropic etch. This zone seems to correspond to the under-etching of the oxide mask and thus to the onset of the etching. On the other hand, the bottom of the cavities is best described by linear slopes, which corresponds to an anisotropic etching. These two slopes form an open angle of about 125° at the bottom of the cavities. This anisotropic character of the etching is probably due to the high dopant concentration of the silicon wafers used. The dopant concentration of standard silicon wafers (resistivity of 15-25 Ω.cm) is indeed around 5-9 10^{14} cm^{-3}, while the dopant concentration in the wafers used is 1-1.5 10^{20} cm^{-3}. Furthermore, it has been shown that the etch rate and etching characteristics of silicon by HNA is dependent on the dopant concentration [49]. However, highly doped silicon is necessary as it allows a smooth interface between the porous layer and the silicon bulk, which is of the utmost importance for optical applications.

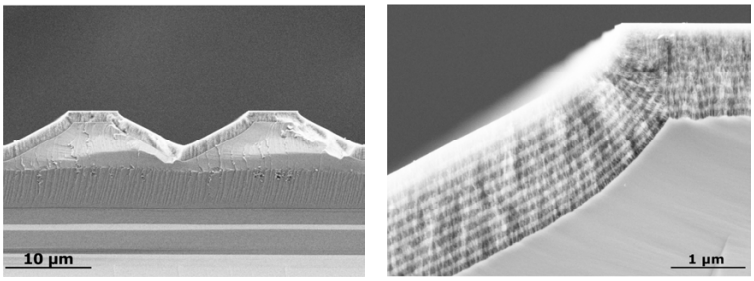

Fig. 3. SEM pictures of the bio-inspired concave porous silicon multilayer structure.

Furthermore, we can observe the high conformity of the electrochemical etching process, with each layer of porous silicon concordant with the geometry of the cavity, conserving therefore the original concave profile.

It is also interesting to compare the porous silicon multilayer of the bio-inspired concave structure to the one of the flat Bragg mirror (Fig. 3 and 4). As expected, we observe similar porous silicon multilayer with layers of high and low porosity. The thickness of each layer, measured by SEM, as well as the porosity and refractive index, measured by spectroscopic liquid infiltration method [50], are given in Table 2.

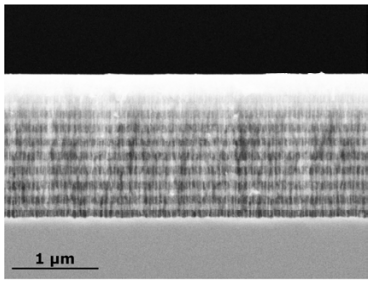

Fig. 4. SEM picture of the flat porous silicon Bragg mirror.

Table 2.Vapor dilutions used during the measurements.

	Layer 1	Layer 2
Current density [mA/cm^2]	12.5	80
Thickness [nm]	65	90
Porosity [%]	32	74
Refractive index	2.10	1.54

3.2 Optical vapor sensing

Optical reflectance spectra of the flat porous silicon Bragg mirror and the bio-inspired porous silicon multilayer can be seen in Fig. 5(a) and (b) respectively for increasing concentrations of ethanol vapor. The related changes in reflectance are shown in Fig. 5(c) and (d), and are defined as $\Delta R(\lambda) = (R_0(\lambda) - R_i(\lambda))/R_0(\lambda)$ with $R_0(\lambda)$ being the reflectance of the sample in dry air at a wavelength λ and $R_i(\lambda)$ the reflectance of the sample exposed to ethanol vapor, in a concentration i ranging from 0% to 100% by step of 25%.

The reflectance of the bio-inspired structure is significantly lower than the one of the flat Bragg mirror (Fig. 5(a)-(b)). This is explained by the specular reflection from the flat Bragg mirror, where all the light is detected by the spectrophotometer and the scattering properties of the bio-inspired structure due to its cavities. Nevertheless, part of the light is detected after multiple reflections in the cavities.

Upon contact with saturated ethanol vapor (100%), the stop-band position is red-shifted by 10.6 nm and 5.0 nm in the cases of the bio-inspired structure and the flat Bragg mirror, respectively (Fig. 5(a)-(b)). As the stop-band shift clearly shows a dependence on the ethanol concentration, the shift for both structures was plotted as a function of ethanol concentration (Fig. 6(a)). In addition to the stop-band shift, the reflectance change $\Delta R(\lambda)$ is also significantly modified. Regardless of the wavelength, its maximal absolute value is four times higher with the bio-inspired structure than with the flat Bragg mirror, and globally it is twice as high (Fig 5(c)-(d)). As we can see, these reflectance changes are mainly due to the edges of the stop-band and Fabry-Pérot fringes.

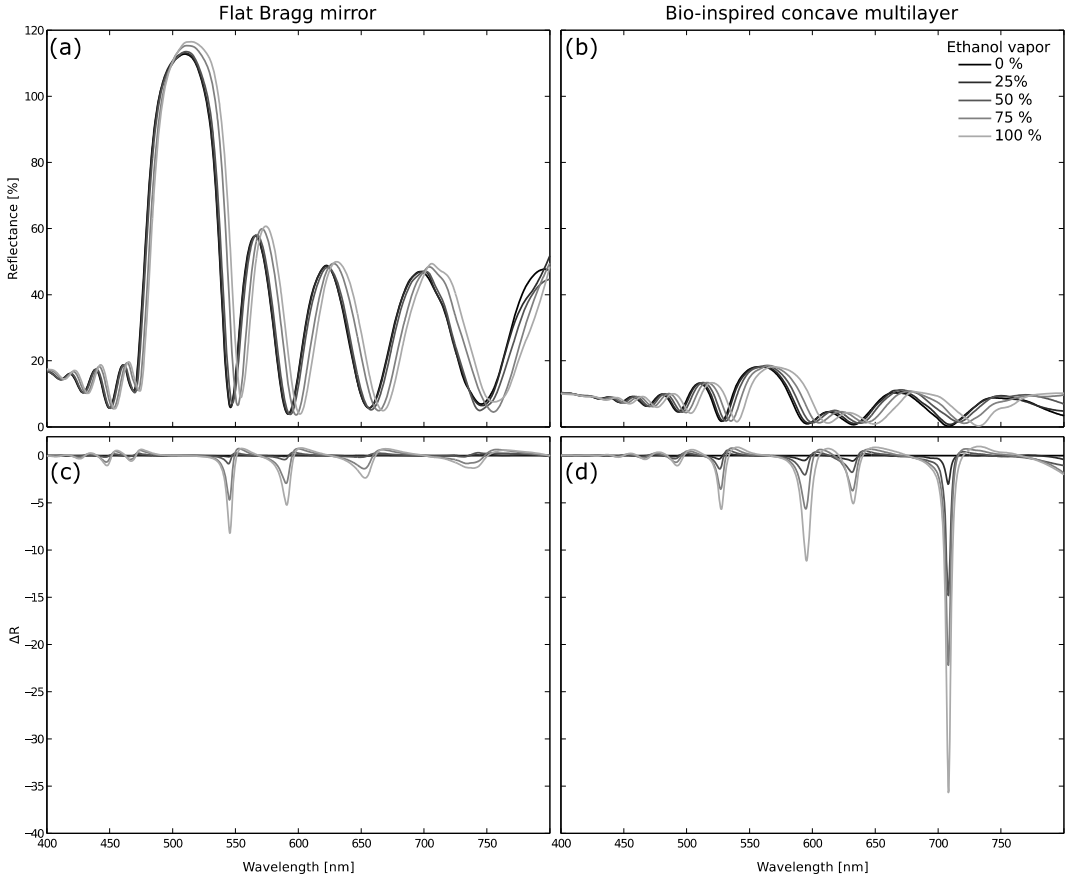

Fig. 5. Reflectance spectra of (a) the flat porous silicon Bragg mirror and (b) the bio-inspired porous silicon multilayer exposed to different concentrations of ethanol vapor and the related reflectance change spectra $\Delta R(\lambda) = (R_0(\lambda) - R_i(\lambda))/R_0(\lambda)$ with the reflectance $R_0(\lambda)$ in dry air and the reflectance $R_i(\lambda)$ from the sample exposed to a given concentration i of ethanol vapor (respectively (c) and (d)).

The sum $\Sigma_\lambda |\Delta R(\lambda)|$ of the reflectance changes $\Delta R(\lambda)$ for wavelengths ranging from 400 nm to 800 nm at a given vapor concentration was found to depend on the vapor concentration for both the flat Bragg mirror and the bio-inspired multilayer (Fig. 6(b)). We observe the same behavior for both structures, while the bio-inspired multilayer exhibits an increased sensitivity to changes in the vapor concentration, which is about two times the response of the flat Bragg mirror, regardless of the vapor concentration.

This increased optical response can be explained by the larger area of the bio-inspired multilayer compared to the flat Bragg mirror while being at non-equilibrium conditions. Indeed, even though at equilibrium the condensation should be comparable for both structures, and thus the stop-band shift, we observe a faster response of the bio-inspired multilayer. This is due to the larger area facilitating the mass transport and providing an efficient surface accessibility [51]. The red shift of the stop-band and the reflectance changes are thus more easily observed for shorter time in the case of the bio-inspired multilayer compared to a flat Bragg mirror.

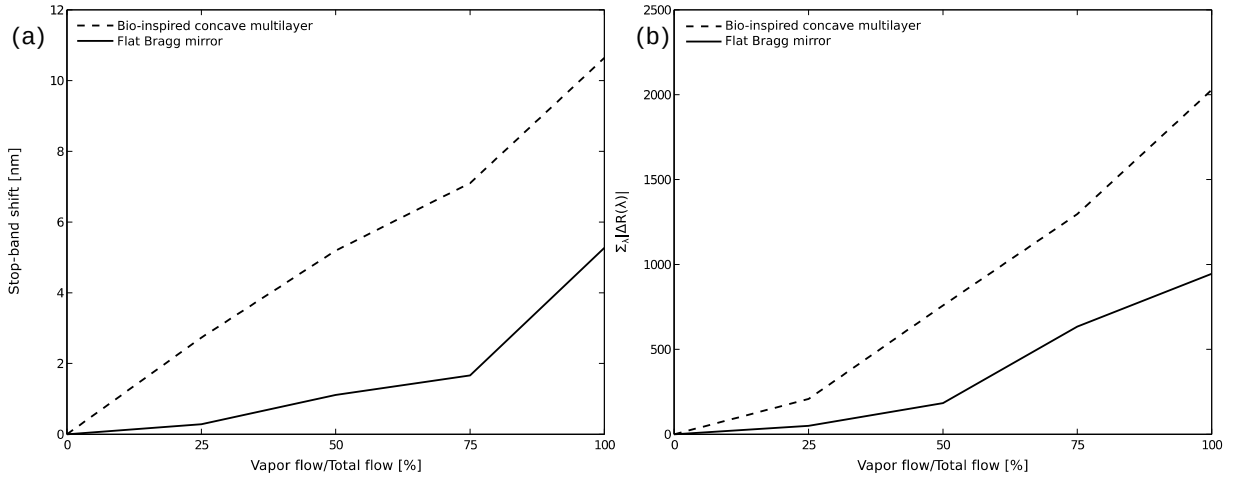

Fig. 6. (a) Value of the stop-band red shift and (b) sum of the reflectance changes for wavelengths ranging between 400 nm and 800 nm as a function of the vapor dilution for the bio-inspired concave structure and the flat porous silicon Bragg mirror.

4. Conclusion

The concave structure of the *Papilio blumei* butterfly wing scales was reproduced using standard microfabrication techniques combined with electrochemical etching to obtain a photonic crystal best described as a concave porous silicon multilayer. This structure optical response to ethanol vapor was compared to a flat porous silicon Bragg mirror, which can be considered as a standard in the literature for optical vapor sensing based on porous silicon. The bio-inspired concave porous silicon multilayer exhibited a significantly higher response than the standard, due to a larger reactive area, which provides a more efficient surface accessibility and leads to improved mass transport properties of the analyte. This allowed an enhanced sensitivity to ethanol vapor while being at non-equilibrium conditions. The bio-inspired sensor showed great potential, as a proof of concept, for the detection of volatile organic compounds. In addition, future research will be led in order to discriminate various chemical species thanks to porous silicon structures' large reactive surface and significant sensitivity to environmental changes.

Acknowledgements

Micro-fabrication processes were performed in Wallonia Infrastructure Nano Fabrication (WINFAB) at UCL. This research was supported by the Belgian National Fund for Scientific Research F.R.S.-FNRS through the Research credit CDR J.0035.13.

J. Rasson was supported by a FRIA fellowship (F.R.S.-FNRS). S. R. Mouchet was supported by F.R.S.-FNRS as a Research Fellow, by Wallonia-Brussels International (WBI) through a Postdoctoral Fellowship for Excellence

program WBI.WORLD and by the Royal Academy of Science, Letters and Fine Arts of Belgium through a grant of the Agathon De Potter Fund.

References

[1] R.A. Potyrailo, H. Ghiradella, A. Vertiatchikh, K. Dovidenko, J.R. Cournoyer, E. Olson, Nat. Photonics 1 (2007) 123-128.
[2] T. Jiang, Z. Peng, W. Wu, T. Shi, G. Liao, Sens. Actuators A 213 (2014) 63-69.
[3] X. Yang, Z. Peng, H. Zuo, T. Shi, G. Liao, Sens. Actuators A 167 (2011) 367-373.
[4] R.A. Potyrailo, T.A. Starkey, P. Vukusic, H. Ghiradella, M. Vasudev, T. Bunning, R.R. Naik, Z. Tang, M. Larsen, T. Deng, S. Zhong, M. Palacios, J.C. Grande, G. Zorn, G. Goddard, S. Zalubovsky, P. Natl. Acad. Sci. USA 110 (2013) 15567-15572.
[5] L.P. Biró, K. Kertész, Z. Vértesy, Z. Bálint, Proc. of SPIE 7057 (2008) 705706.
[6] J. Huang, X. Wang, Z.L. Wang, Nano Lett. 6 (2006) 2325-2331.
[7] S. Zhu, D. Zhang, Z. Chen, J. Gu, W. Li, H. Jiang, G. Zhou, Nanotechnology 20 (2009) 315303.
[8] S. Kang, T. Tai, T. Fang, Curr. Appl. Phys. 10 (2010) 625-630.
[9] X. Liu, S. Zhu, D. Zhang, Z. Chen, Mater. Lett. 64 (2010) 2745-2747.
[10] F. Liu, Y. Liu, L. Huang, X. Hu, B. Dong, W. Shi, Y. Xie, X. Ye, Opt. Commun. 284 (2011) 2376-2381.
[11] F. Liu, W. Shi, X. Hu, B. Dong, Opt. Commun. 291 (2013) 416-423.
[12] M.R. Weatherspoon, Y. Cai, M. Crne, M. Srinivasarao, K.H. Sandhage, Angew. Chem. Int. Edit. 47 (2008) 7921-7923.
[13] W. Peng, S. Zhu, W. Wang, W. Zhang, J. Gu, X. Hu, D. Zhang, Z. Chen, Adv. Funct. Mater. 22 (2012) 2072-2080.
[14] S. Zhu, X. Liu, Z. Chen, C. Liu, C. Feng, J. Gu, Q. Liu, D. Zhang, J. Mater. Chem. 20 (2010) 9126-9132.
[15] O. Poncelet, G. Tallier, S.R. Mouchet, A. Crahay, J. Rasson, R. Kotipalli, O. Deparis, L.A. Francis, Bioinspir. Biomim. 11 (2016) 036011.
[16] A. Saito, Y. Miyamura, Y. Ishikawa, J. Murase, M. Akai-Kasaya, Y. Kuwahara, Proc. of SPIE 7205 (2009) 720506.
[17] K. Watanabe, T. Hoshino, K. Kanda, Y. Haruyama, S. Matsui, Jpn. J. Appl. Phys. 44 (2005) L48-L50.
[18] M. Aryal, D.-H. Ko, J.R. Tumbleston, A. Gadisa, E.T. Samulski, R. Lopez, J. Vac. Sci. Technol. B 30 (2012) 061802.
[19] R.H. Siddique, S. Diewald, J. Leuthold, H. Hölscher, Opt. Express 21 (2013) 14351-14361.
[20] R.H. Siddique, A. Faisal, R. Hünig, C. Bartels, I. Wackers, U. Lemmer, H. Hölscher, Proc. of SPIE 9187 (2014) 91870E.
[21] A. Saito, S. Yoshioka, S. Kinoshita, Proc. of SPIE 5526 (2004) 188-194.
[22] A. Saito, M. Nakajima, Y. Miyamura, K. Sogo, Y. Ishikawa, Y. Hirai, Proc. of SPIE 6327 (2006) 63270Z.
[23] K. Chung, S. Yu, C.-J. Heo, J.W. Shim, S.-M. Yang, M.G. Han, H.-S. Lee, Y. Jin, S.Y. Lee, N. Park, J.H. Shin, Adv. Mater. 24 (2012) 2375-2379.
[24] K. Chung, J.H. Shin, J. Opt. Soc. Am. A 30 (2013) 962-968.
[25] B. Song, S.C. Eom, J.H. Shin, Opt. Express 22 (2014) 19386-19400.
[26] W. Wang, W. Zhang, X. Fang, Y. Huang, Q. Liu, J. Gu, D. Zhang, Sci. Rep. 4 (2014) 5591.
[27] Y.-Y. Diao, X.-Y. Liu, Opt. Express 19 (2011) 9232-9241.
[28] P. Vukusic, J.R. Sambles, C.R. Lawrence, Nature 404 (2000) 457.
[29] P. Vukusic, J.R. Sambles, C.R. Lawrence, G. Wakely, Appl. Optics 40 (2001) 1116-1125.
[30] F. Liu, G. Wang, L. Jiang, B. Dong, J. Opt. 12 (2010) 065301.
[31] D.P. Gaillot, O. Deparis, V. Welch, B.K. Wagner, J.P. Vigneron, C.J. Summers, Phys. Rev. E 78 (2008) 031922.
[32] Z. Zhang, K. Yu, L. Lou, H. Yin, B. Li, Z. Zhu, Nanoscale 4 (2012) 2606-2612.
[33] W. Zhang, D. Zhang, T. Fan, J. Gu, J. Ding, H. Wang, Q. Guo, H. Ogawa, Chem. Mater. 21 (2009) 33-40.
[34] T. Saison, C. Peroz, V. Chauveau, S. Berthier, E. Sondergard, H. Arribart, Bioinspir. Biomim. 3 (2008) 046004.
[35] M. Kolle, P.M. Salgard-Cunha, M.R.J. Scherer, F. Huang, P. Vukusic, S. Mahajan, J.J. Baumberg, U. Steiner, Nat. Nanotechnol. 5 (2010) 511-515.
[36] M.-L. Lo, W.-H. Li, S.-Z. Tseng, S.-H. Chen, C.-H. Chan, C.-C. Lee, J. Nanophotonics 7 (2013) 073597.
[37] M. Crne, V. Sharma, J. Blair, J.O. Park, C.J. Summers, M. Srinivasarao, Europhys. Lett. 93 (2011) 14001.
[38] O. Poncelet, G. Tallier, P. Simonis, A. Cornet, L.A. Francis, Bioinspir. Biomim. 10 (2015) 026004.
[39] I.A. Levitsky, Sensors 15 (2015) 19968-19991.
[40] S.E. Létant, M.J. Sailor, Adv. Mater. 12 (2000) 355-359.
[41] J. Gao, T. Gao, M.J. Sailor, Appl. Phys. Lett. 77 (2000) 901-903.
[42] A.M. Ruminski, B.H. King, J. Salonen, J.L. Snyder, M.J. Sailor, Adv. Funct. Mater. 20 (2010) 2874-2883.
[43] M. Rocchia, A.M. Rossi, G. Zeppa, Sens. Actuators B 123 (2007) 89-93.
[44] L.N. Acquaroli, R. Urteaga, R.R. Koropecki, Sens. Actuators B 149 (2010) 189-193.
[45] P.A. Snow, E.K. Squire, P.S.J. Russel, L.T. Canham, J. Appl. Phys. 86 (1999) 1781-1784.
[46] L. De Stephano, I. Rendina, L. Moretti, A.M. Rossi, Mater. Sci. Eng. B 100 (2000) 271-274.
[47] H.-J. Kim, Y.-Y. Kim, K.-W. Lee, H. Cheng, H.D. Han, Physica B 406 (2011) 1536-1541.
[48] S.R. Mouchet, T. Tabarrant, S. Lucas, B.-L. Su, P. Vukusic, O. Deparis, Opt. Express 24 (2016) 12267-12280.
[49] K.E. Petersen, Proc. of the IEEE 70 (1982) 420-457.
[50] E. Segal, L.A. Perelman, F. Cunin, F.D. Renzo, J.-M. Devoisselle, Y.Y. Li, M.J. Sailor, Adv. Funct. Mater. 17 (2007) 1153-1162.
[51] X. Guo, H. Zhou, D. Zhang, T. Fan, RSC Adv. 4 (2014) 3748-3752.